Proceedings of the Eighth Meeting of the International Collaboration on Advanced Neutron Sources (ICANS-VIII)
8-12 July 1985, Rutherford Appleton Laboratory Report RAL-85-110

SPECIALISED NEARELASTIC SPECTROMETER FOR RELAXATIONS IN ATOMIC LIQUIDS

by P.A. Egelstaff

Physics Department

University of Guelph, Guelph, Ontario

Abstract

For the study of gases, liquids and glasses it is useful to make inelastic scattering measurements at low q using neutrons of ~1Å. The case for this type of research is demonstrated through the recent analysis[1] of inelastic scattering data on dense gases taken at the 1N4 spectrometer. Until the development of the new pulsed neutron sources, the combination of reasonable resolution with reasonable counting rates in this regime was difficult or impossible to achieve. However by exploiting the new sources it seems possible to open up this field with a new spectrometer for nearelastic scattering, and a prototype instrument is described.

Introduction

The study of collective excitations in dense gases, liquids and glasses has a long history during which the importance of the transition regime between hydrodynamic behaviour and a collision dominated regime has been stressed. There is an extensive theoretical and experimental literature and several controversies are unresolved.

In terms of the dynamic structure factor, $S(q,\omega)$ the transition regime occurs for $0.1 < q < 0.6$ A^{-1} and $\omega \sim vq$, where v is the velocity of sound. These boundaries are not clearly defined and vary from sample to sample, but for many materials lie beyond the capabilities of commonly used neutron spectrometers (e.g. the 1N4 at the I.L.L. and the conventional 3-axis instruments). Only a few demonstration experiments have been attempted so far. One reason for this is the coupling between q and ω in neutron experiments, which is shown in figure 1. In this figure the ratio $y = \omega/v_n q$ (ω/q is the velocity of sound when a mode is observed and v_n is the neutron velocity) is plotted against the ratio (x) of the momentum transfer ($\hbar q$) to the neutrons momentum (mv_n). For this plot a mode having an approximately linear ω-q relationship will correspond to y=constant. Since the range of q is pre-determined, x cannot be large unless the incident neutrons velocity (v_n) is small: but in this case y will be large and outside the experimentally accessible range shown in the figure. Thus, as is well known, a relatively large neutron velocity is needed for these experiments: for practical purposes it should be greater than v. Because v varies between ~ 700 m/s for gases and ~ 3000 m/s for low temperature glasses, a reasonable choice is $v_n \sim 5000$ m/s ($\lambda \sim 1$Å). To reduce the experimental difficulties a lower velocity could be used for gaseous samples, and so an instrument offering a few fixed wavelengths in the 1 to 2 Å range would be suitable. The hatched area in figure 1 shows the area bounded by these requirements on q, v and v_n. The main point is that angles less than 5^o are needed.

The resolution requirements are also rather stringent, because the mode frequency is $\sim 10^{12}$ $rads^{-1}$ for gases and a resolution width of ~ 1/10 of this frequency is needed. For example, a conventional time-of-flight experiment using 1 Å neutrons would involve ~ 15 m paths with time channels ~ 2.5 μsec. However if we ask that the 5 degree angular range is divided into ~ 0.1^o intervals, the sample dimensions would be ~ 2 cms at 15 m. Fortunately the samples in this field may be fabricated conveniently in this

size. Moreover a position sensitive detector of dimensions ~ 1 m diameter and ~ 2 cm resolution is a reasonable possibility. Thus although these characteristics are unusual, they are not inconceivable for an intense pulsed neutron source and modern instrument techniques.

Other details of a proposed instrument will be given later, but meanwhile a brief theoretical background will be given.

2. Brief Theory of R.A.L. via S(Q,ω)

The hydrodynamic theory of relaxations in atomic liquids may be used to derive an expression for S(q,ω). This expression, valid for q → o, is the sum of three Lorentzians; one centered on ω = o related to non-propagating modes and one each centered at ω = ± vq related to propagating sound modes. For larger values of q a generalised version of this expression has been derived in many papers, and may be written:

$$S(q,\omega) = \frac{1}{\pi} \frac{\frac{kT}{M} q^2 \, \mathrm{Re}[M(q,\omega)]}{\left| \omega_o^2 - i\omega \, M(q,\omega) - \omega^2 \right|^2} \qquad (1)$$

where $\omega_o^2 = kT\, q^2/MS(q)$, and S(q) is the static structure factor. M(q,ω) is the Laplace transform of the memory function for the current-current correlation function in one form of the theory, and is the generalised viscous damping function for propagating modes in another form. Egelstaff and Gläser[1,2] rewrite equation (1) in terms of a normalised frequency $x = \omega/\omega_o$ and a normalised daming function, σ, i.e.:-

$$S(q,x) = \frac{S(q)}{\pi} \cdot \frac{\sigma_1/c}{\left| \frac{\sigma}{c}(1-x^2) + ix \right|^2} \qquad (2)$$

where $S(q,\omega) = \omega_o S(Q,\omega)$, $\sigma = \omega_o c/M^*(q,\omega)$ and $c = \pi\, S(q,x=o)/S(q)$. This form makes it clear that S(q,x) depends on only two functions σ_1/c and σ_2/c (where $\sigma = \sigma_1 + i\sigma_2$). In a simple model where equation (1) is the sum of three Lorentzians having ω-independent parameters which satisfy the zero, second and fourth frequency moments of S(q,ω) we find $\sigma = 1 + i\omega\tau$ where τ is

an unknown constant. If we make no corrections to this model for the very high frequency behaviour of $S(q,\omega)$ then τ may be related to the fourth moment, and the memory function is an exponential function of time. Lovesey[3] employed this model and called it "a simple visco-elastic model." An advantage of the function $S(q,x)$ - equation 2 - is that σ_1 and σ_2 are weakly dependent on ω, in contrast to the stronger ω-dependence of $M(q,\omega)$ for example. Thus the approximation $\sigma = 1 + i\omega\tau$ is a good first approximation, and it would be useful to make measurements and perform analyses of sufficient precision that departures from this approximation are readily seen.

The inversion of $S(q,x)$ to find σ is, in principle, straightforward[1]. However in practice serious errors arise in the necessary Fourier-Laplace transform procedure for three reasons:-

(i) the experimental data extend over a finite ω-range

(ii) the errors tend to be large on a relative scale, at high ω,

(iii) equation (1) is a classical equation, and can be used only for

$$\hbar\omega \lesssim kT/3.$$

It has been shown[1] that the range of ω over which $M(q,\omega)$ exhibits significant intensity is considerably wider than that for $S(q,\omega)$, and therefore these three restrictions limit ω in real data to a "near-elastic" range as far as $M(q,\omega)$ is concerned. Thus we need to invert $S(q,x)$ to σ in frequency space using a relatively narrow or nearelastic range of ω. This problem was solved in reference 1, and details will not be given here.

The principal feature considered in many of the papers written during the long history of this subject, is the damping of the propagating modes (particulary the magnitude of the damping) and often this is related to subjective criteria. By using the quantities σ_1/c and σ_2/c derived from $S(Q,\omega)$ a simple solution for the damping problem is obtained. In reference 1 (equation 33b) it is shown that the ratio ω_s/Z_s (where ω_s is the real and Z_s the imaginary part of acomplex frequency for the mode) is determined by the point $[\sigma_1/c;\ \sigma_2^o/c]$ in figure 2. Thus without discussing subjective features, such as the shape of $S(Q,\omega)$, a quantitative measurement of a

meaningful ratio is possible. The experimentally observed behaviour of ω_s/Z_s v.s. q, and the behaviour of σ_1 or σ_2^o v.s. q can, in some cases, be complicated, and examples will be given in the next section. While present experiments show structure as a function of q, it is evident that not all the structure has been observed and further data at lower q are required. This is particularly interesting since some of the structural features are not correlated with those in S(q).

3. Illustrative examples of the relaxation parameters

The scale factor appearing in equation (2) is $c = \pi\ S(q,o)/S(q)$ and may be evaluated easily from experimental data. Gläser and Egelstaff[2] present a summary of five sets of experimental data, and compare them with the predictions of a simple 'collision model.' The argon and krypton data are shown in figure 3 (see table 1 also). It can be seen that these data show structure as a function of q, which is not included in the simple model, but that the general level for $q > 1\ \text{Å}^{-1}$ is accounted for approximately. When q is less than $1\ \text{Å}^{-1}$, the collison model fails because collective effects become important and there is a transition towards the hydrodynamic regime. The data displayed extend to $q \sim 0.4\ \text{A}^{-1}$, but their quality is not satisfactory for $q < 0.6\ \text{A}^{-1}$. Thus the transition is not covered by these data.

Figure 4 is a plot of σ_1 v.s. q for argon and krypton (see lines 2 and 4 of table 1). For $\omega \sim 0.4\ \omega_o$ it does not differ significantly from its value at $\omega = o$ (i.e. $\sigma_1 = 1$). However for $\omega \sim 2\ \omega_o$ and $q < 1\ \text{A}^{-1}$, σ_1 is greater than unity. In the hydrodynamic limit[1] it is $\sigma_1(\omega=\omega_o) = 1 + \nu C_v[D_T(C_p-C_v)]^{-1}$ where ν is the kinematic viscosity, D_T is the thermal diffusivity and C_v and C_p are the specific heats at constant volume and pressure respectively. This limit is much larger than the values given in figure 4, so that we expect a sharp increase at lower q. At figure 5, σ_2/ω is plotted as a function of q, and it can be seen that between $\sim 0.4\omega_o$ and $\sim 2\omega_o$, there is little change. In figure 6, the values of ω, corresponding to the data of figure 5 are shown. The magnitude corresponds

to times less than 0.1 ps., while the lowest values are comparable to h/kT. These small times indicate that M(Q,t) has some structure as a function of t, so that the area is small (σ_2 at low ω is proportional to this area). In the hydrodynamic regime σ_2/ω (for low ω) = $[D\ q^2]^{-1}$, and again we are clearly not yet at this limit. The structure in this function is fairly weak.

Thus measurements to lower q would cover some interesting changes in magnitude and possibly more structure in this function. It is interesting to calculate the value of σ_2 as $\omega \to \infty$, using formula (6) of reference 1. For this purpose the fourth frequency moment of $S(q,\omega)$ is required, and for the argon data this has been taken from reference 4. These data show less variation with q than the low ω data and some increase in σ_2 at high (beyond the range of measurement) is indicated. However the error on the determination of the fourth moment is large and thus the magnitude of the increase is not well determined.

It is well known that at high q and at low q we have satisfactory theories, and the diagrams in this section show that while present data merges onto the high q theory, it does not extend low enough to merge onto the low q theory.

4. A Specialised Nearelastic Spectrometer

In the previous two sections the case for studying the nearelastic region (i.e. $\hbar\omega < kT/3$) for krypton and argon when $0.1 < q < 1\ A^{-1}$ was developed. It may also be argued that this region of (q,ω) space is important for other materials and in general any "average energy resonance excitation" may fall into this category (including biological materials and composites). Thus a spectrometer designed to cover this region would be useful, and with the advent of powerful pulsed neutron sources it has become possible to build one. Figure 7 shows the layout for such a spectrometer. To achieve the high energy resolution it is necessary to employ a short pulse of 1 Å neutrons, and for this reason a 95 K methane moderator would be more useful than a room temperature one. Initially the moderator pulse could be employed but later an extra chopper near the source, to sharpen the

pulse, should be added to the design in figure 7. As indicated in the introduction flight paths of about 15 m are required.

It is proposed to use conventional 'reactor type' techniques to displace the detectors from the main beam and to remove the energetic component from the spectrum. Thus a stationary graphite crystal is used to deflect (00ℓ) reflections by 17^{o} for 002 or 35^{o} for 004, and a saphire filter is used to remove short wavelength components. Then a Fermi chopper having a 2.5 μsec pulse width is placed just before the sample to improve the energy resolution of the pulse falling on the sample and to remove other orders. A large position sensitive detector (100 cms square) - similar to those used in conventional SANS at reactors - is set up 15 m from the sample. However to allow for slightly larger angle deflections it may be moved on a track (roughly parallel to the incident beam) so that deflections to one side of the beam passing through the sample may be observed in addition to the conventional SANS arrangement. Finally since most of the incident beam passes through the graphite crystal, the same beam may be used for (at least) two other similar spectrometers employing slightly different wavelengths. It may be useful to design the system so that any wavelength may be chosen from the set, 2.0, 1.8, 1.6, 1.4, 1.2 or 1.0 Å. It does not seem necessary to scan the wavelength so that a choice from a fixed set would suffice to optimise the intensity for any given sample.

To estimate the counting rate it may be useful to compare the performance with that of 1N4 at the I.L.L. Grenoble (in its original form with 4 m paths). For the same size sample at both spectrometers the geometry is changed by a factor of ~ 1/50, while the energy resolution width is reduced by ~ 1/5 and the detector area per (low) angle is increased by ~ 5 times. Thus the net effect is a decrease in throughput by ~ 50, which may be offset by the more powerful source giving higher intensity at 1 Å.

5. Conclusions

The longstanding case for the study of excitations in the low q and nearelastic ω range has been restated, giving emphasis to the problem of

excitations in simple fluids. These particular problems have a long history stretching over 100 years and have often been a source of controversy. By exploiting the new generation of pulsed sources and building a new spectrometer to study this region, and also by using the newly developed techniques of interpretation it may be possible to resolve some of these long standing problems. Moreover such an instrument would be very productive, and its use could be extended to other materials and problems which have an interesting history as well.

Acknowledgement

I would like to thank Dr. W. Gläser for helpful discussions on the subject of this paper.

References

(1) Egelstaff P.A. and Gläser W. Phys. Rev. A 31, 3802, (1985).

(2) Gläser W. and Egelstaff P.A. "Properties of Collective Modes in Fluids - Experimental Results". To be published.

(3) Lovesey S.W. J. Phys. C. 6, 1856, (1973).

(4) van Well A.H., Verkerk P., de Graaf L.A., Suck J-B, and Copley J.R.D. Phys. Rev. A 31, 3391, (1985).

(5) Egelstaff P.A., Gläser W., Litchinsky D., Schneider E. and Suck J-B. Phys. Rev. A 27, 1106, (1983).

Table 1

Summary of Experiments

Case	Element	Temp. K	Density atoms/nm^3	Ref.	Mean Free Path ℓ(Å)	Wave-length(Å)	$\sqrt{\frac{kT}{M}}$ Å/ps.	H.S. dia d(Å)	ρd^3
1	Ar	120	20.1	4	0.25	0.60	1.666	3.4	.79
2	Ar	120	17.6	4	0.35	0.60	1.666	3.4	.69
3	Kr	297	13.8	5	0.48	0.24	1.717	3.53	.61
4	Kr	297	10.6	5	0.8	0.24	1.717	3.53	.47

Notes: H.S. dia is the effective hard sphere diameter deduced from a fit to the position and peak height of the principal peak in S(Q).

The wavelength is calculated for velocity $V_o = \sqrt{kT/M}$.

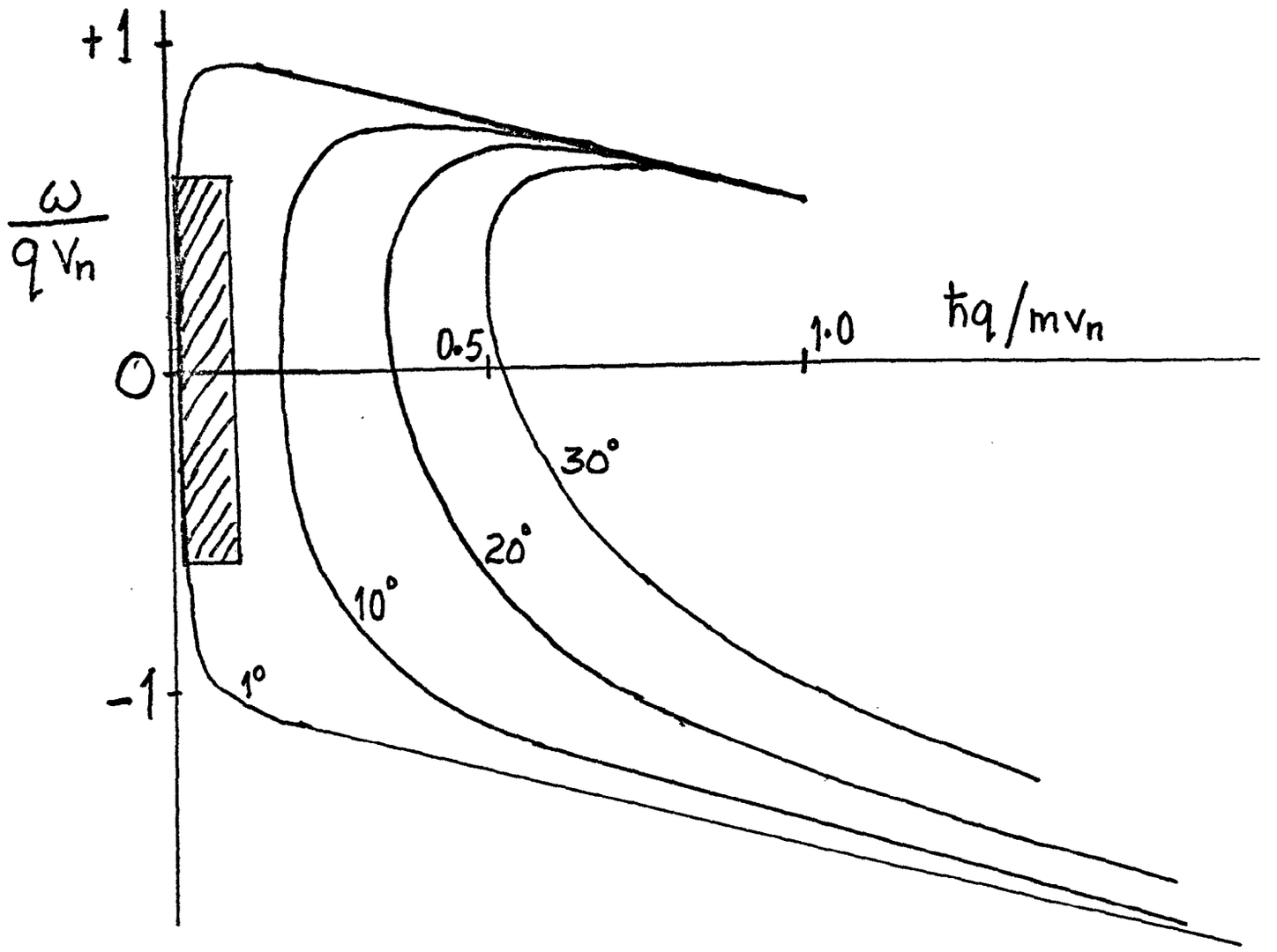

1. An ω-q diagram for nearelastic scattering. The ratio (ω/qv_n) where v_n is the neutron velocity is plotted against the momentum ratio $\hbar q/mv_n$ for several values of θ. The hatched region shows the part of the diagram discussed in this paper.

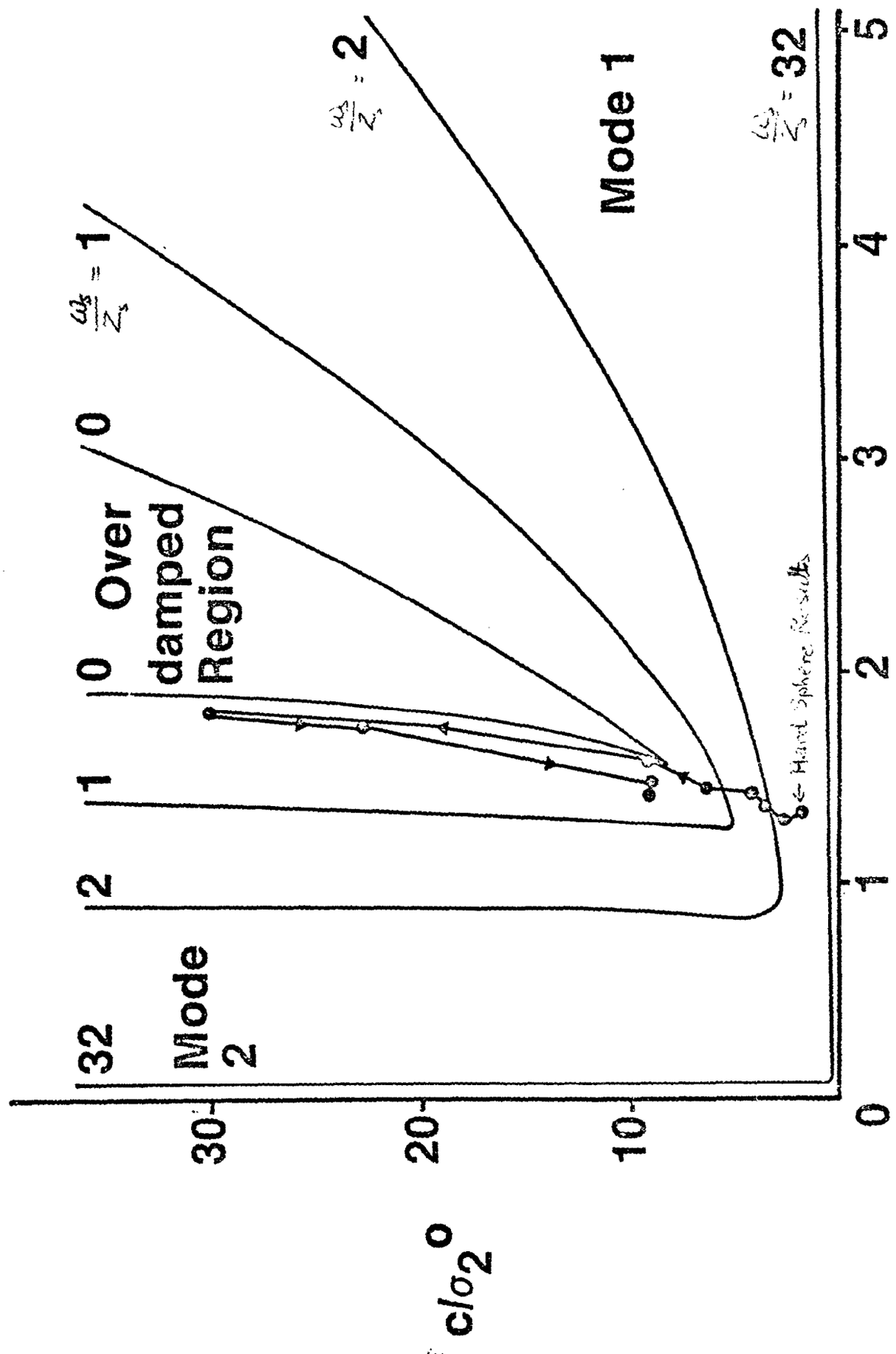

2. Propagating mode diagram: the ratio c/σ_1 is plotted against c/σ_2 for different choices of ω_s/Z_s, where the mode frequency is $\omega_s + iZ_s$.

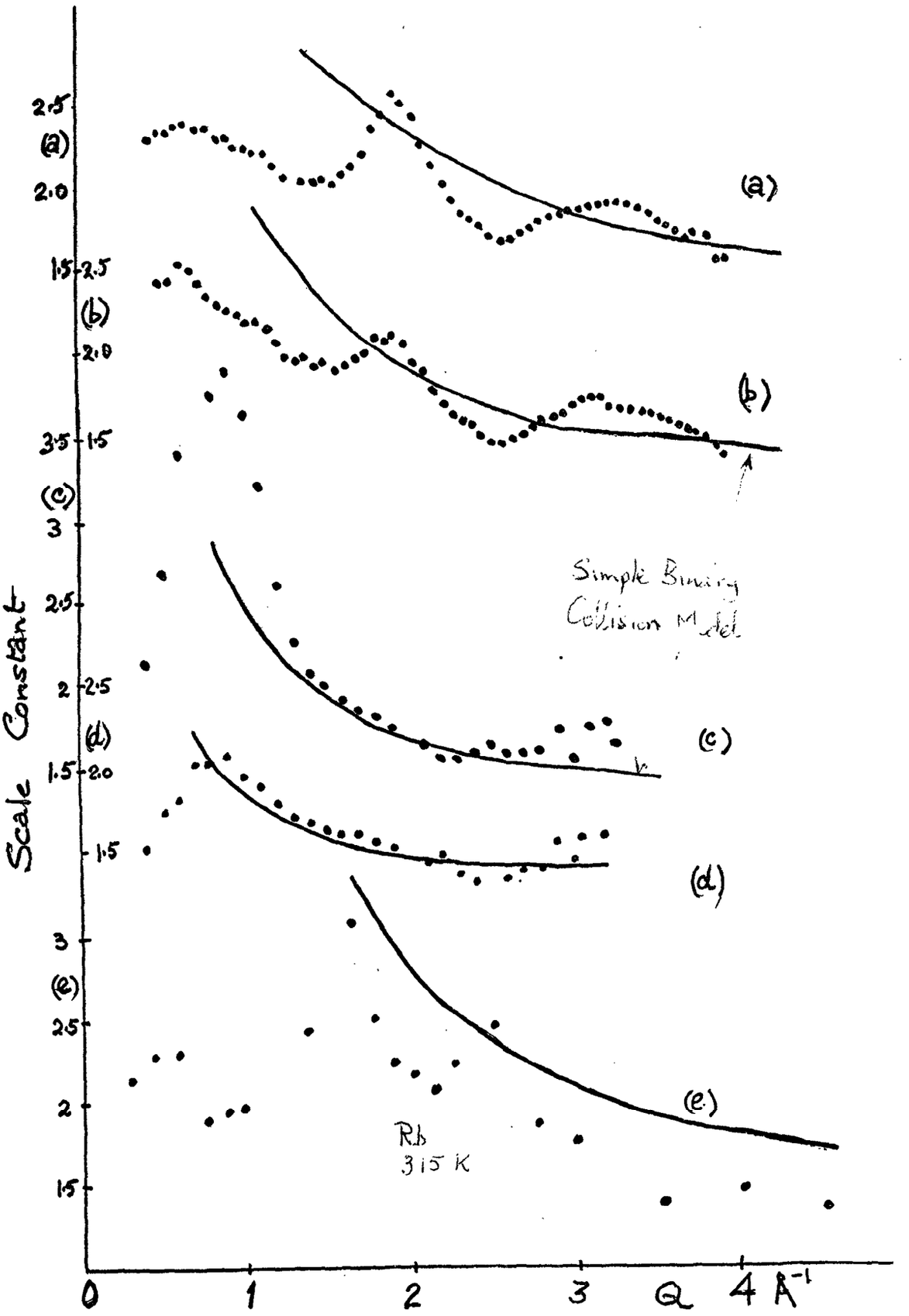

3. The scale constant c, appearing in equation 2, is plotted as a function of q for five sets of experimental data.[2] Details are given in table 1.

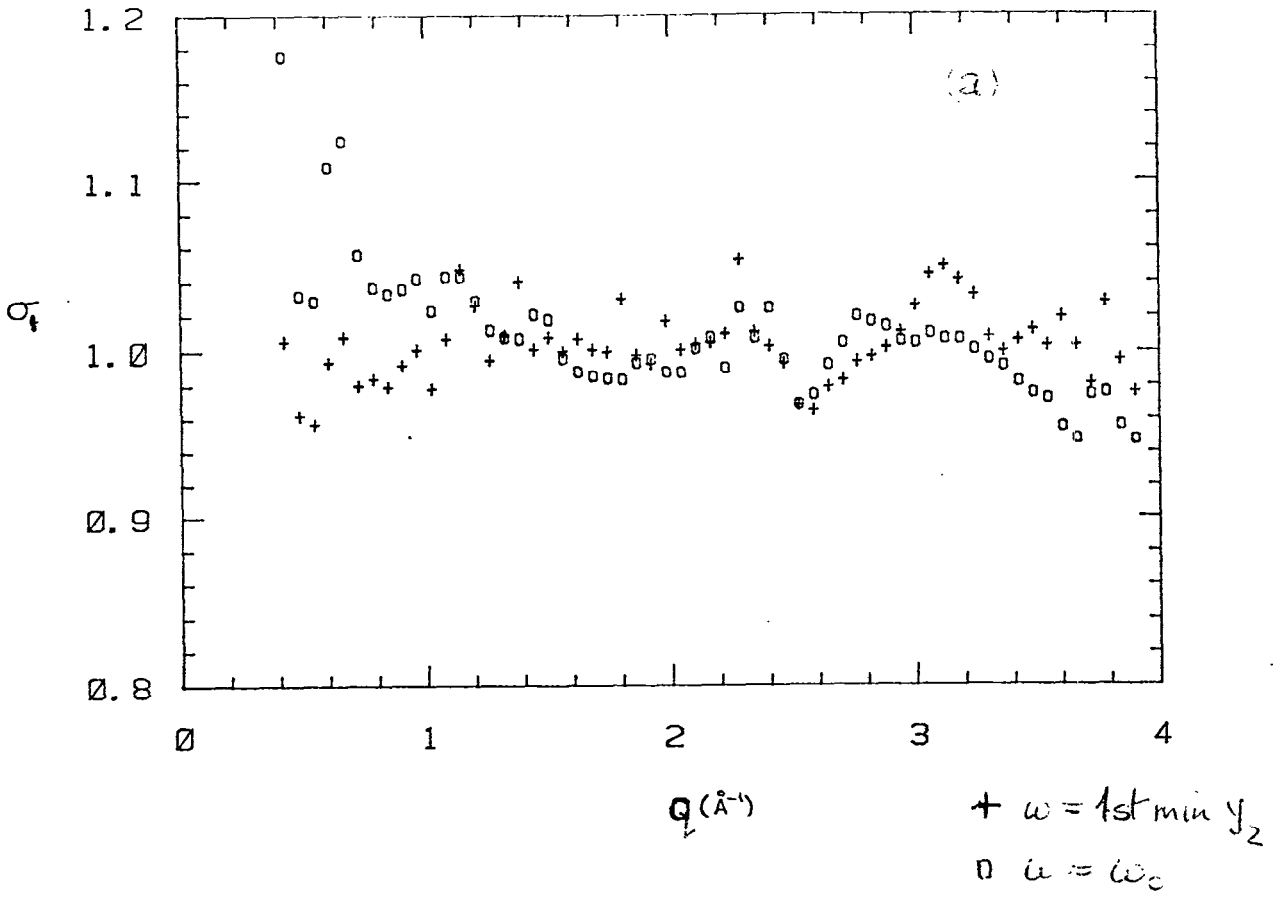

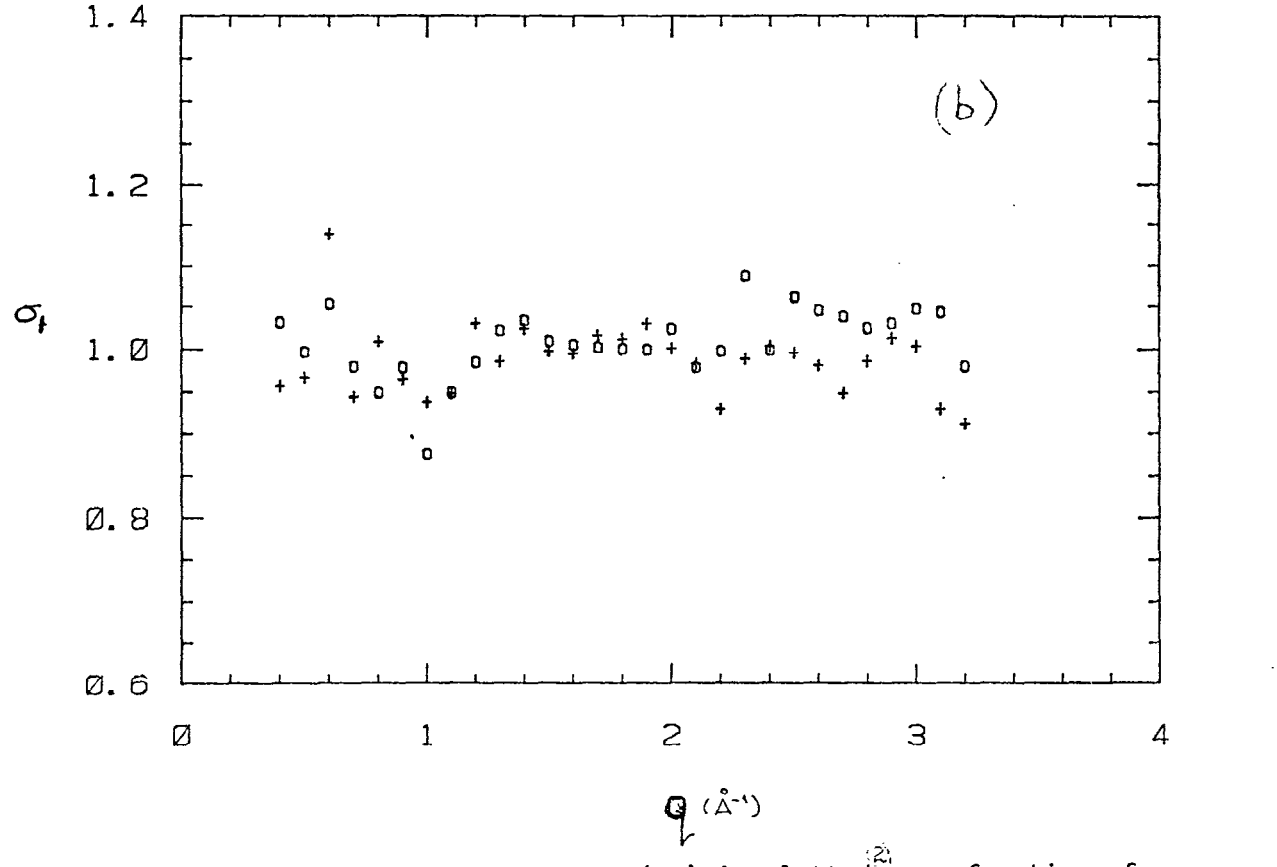

4. The real part of the damping function (σ_1) is plotted as a function of q for the (a) Ar and (b) Kr experiments 2 and 4of table 1. The symbols indicate two different values of ω, the lowest ω shown in figure 6 and ω_0.

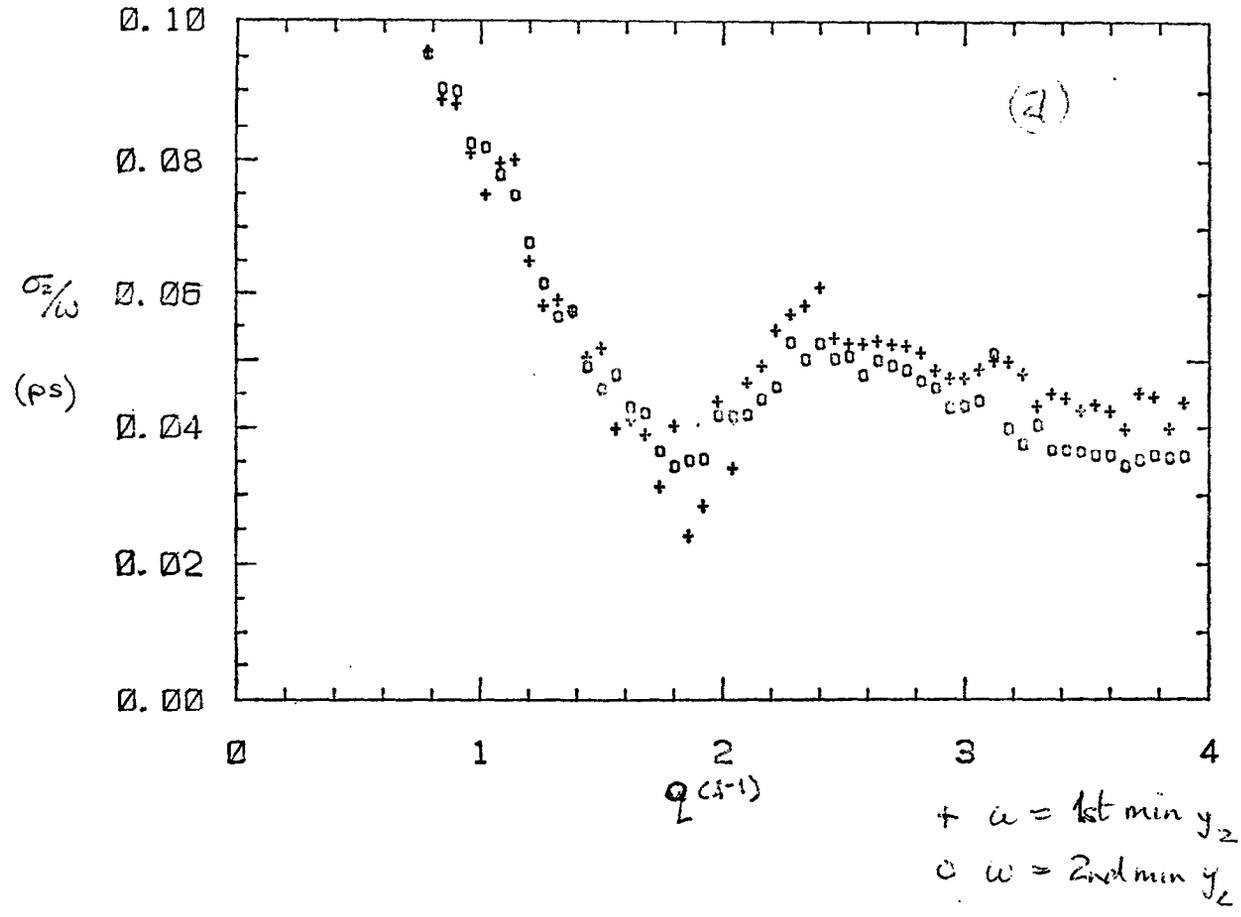

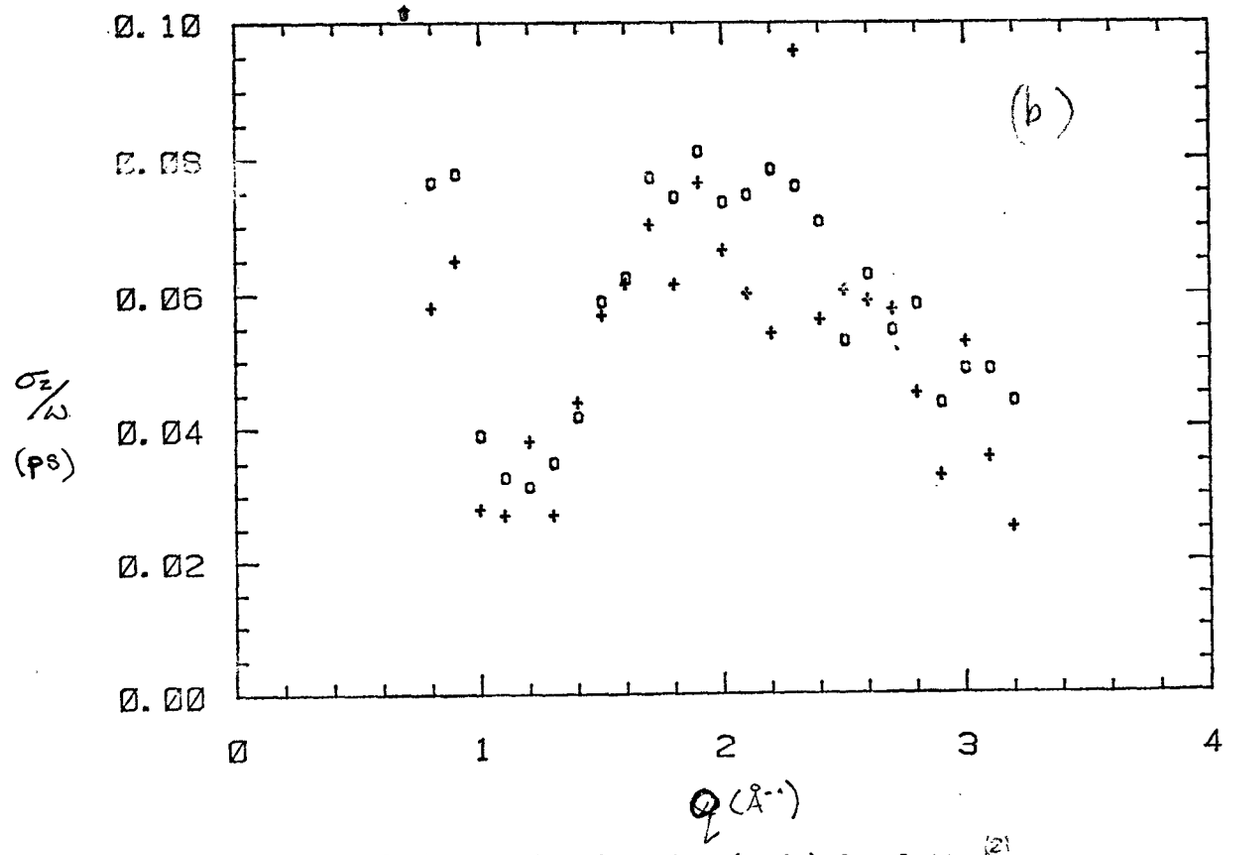

5. The imaginary part of the damping function (σ_2/ω) is plotted[21] as a function of q for the (a) Ar and (b) Kr experiments 2 and 4 of table 1. The symbols indicate two different values of ω shown in figure 6.

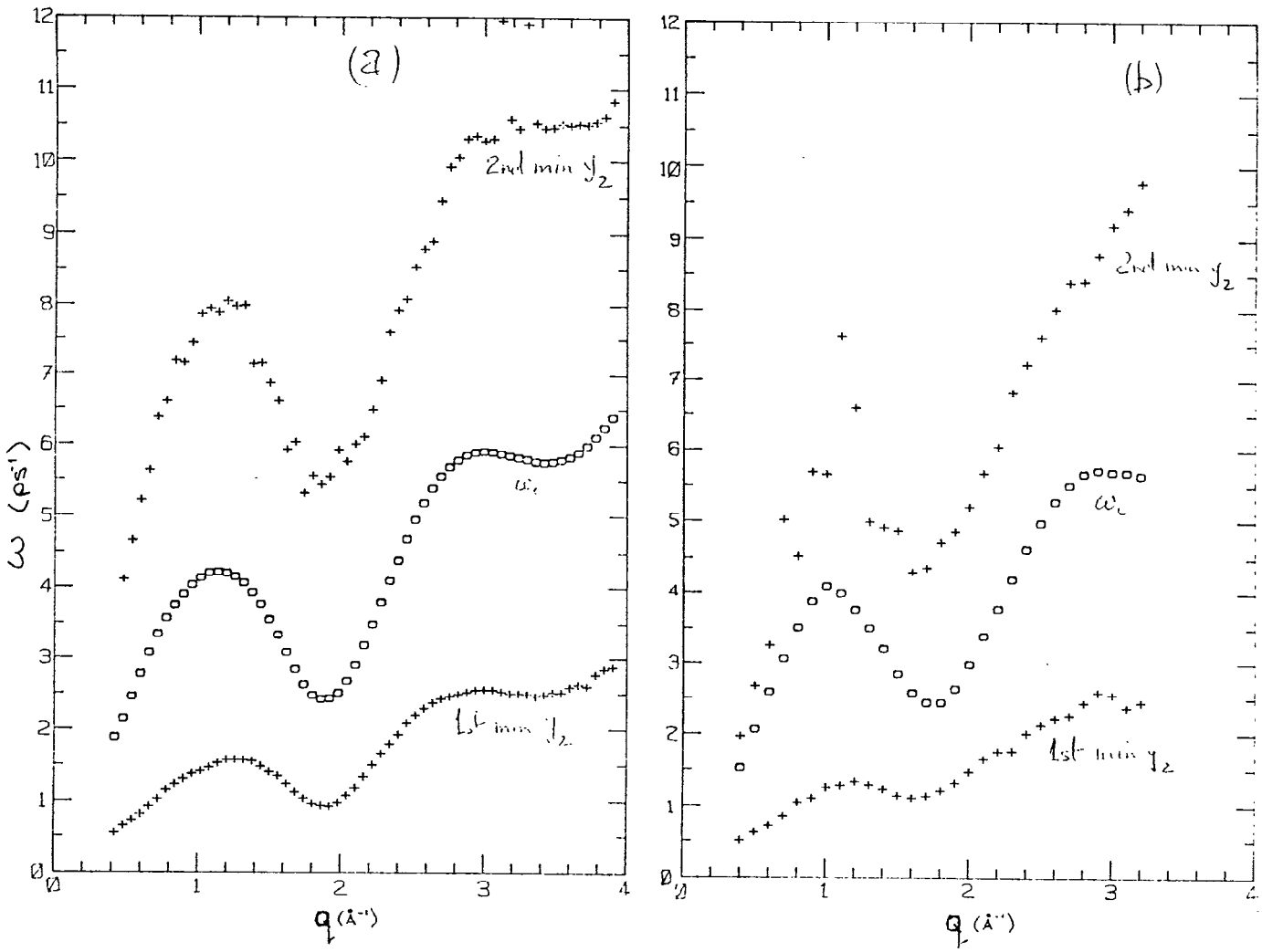

6. The values of ω for which minima are found[2] compared to $\omega_o = q\sqrt{\frac{kT}{MS(q)}}$. The data of figure 5 are for the upper and lower curves shown here.

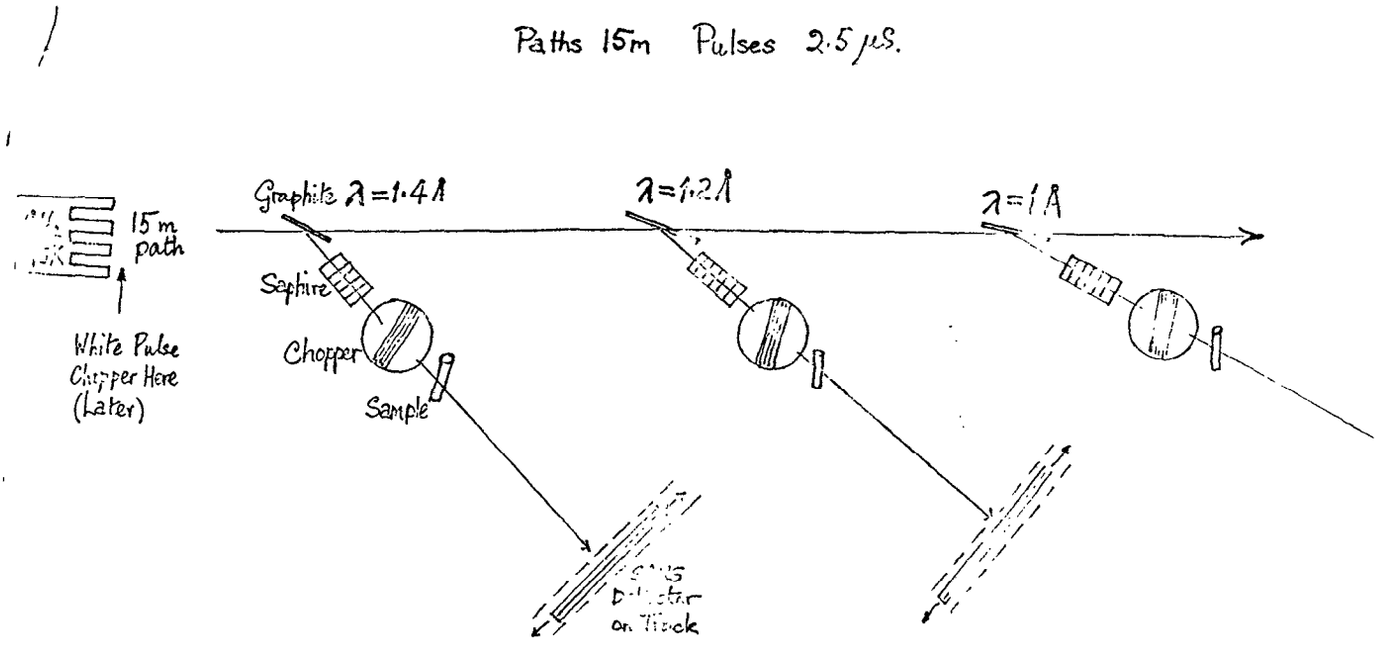

7. An SNS for RAL and AERE. A simple layout diagram for the specialised nearelastic spectrometer for relaxations in atomic liquids and for average energy resonance excitations as described in section 4.